FEATURE ARTICLE

Check for updates

Copper nanoclusters: emerging photoredox catalysts for organic bond formations

Arunachalam Sagadevan,† Kathiravan Murugesan,† Osman M. Bakr 🄳 and Magnus Rueping 🄳 *

Advancements in fine chemical synthesis and drug discovery continuously demand the development of new and more efficient catalytic systems. In this regard, numerous transition metal-based catalysts have been developed and successfully applied in industrial processes. However, the need for innovative catalyst systems to further enhance the efficiency of chemical transformations and industrial applications persists. Metal nanoclusters (NCs) represent a distinct class of ultra-small nanoparticles (<3 nm) characterized by a precise number of metal atoms coordinated with a defined number of ligands. This structure confers abundant unsaturated active sites and unique electronic and optical properties, setting them apart from conventional nanoparticles or bulk metals. The well-defined structure and monodisperse nature of NCs make them particularly attractive for catalytic applications. Among these, copper-based nanoclusters have emerged as versatile and sustainable catalysts for challenging organic bond-forming reactions. Their unique properties, including natural abundance, accessible oxidation states, diverse ligand architectures, and strong photophysical characteristics, contribute to their growing prominence in this field. In this review, we discuss the photocatalytic activities of Cu-based nanoclusters, focusing on their applications in cross-coupling reactions (C–C and C–N), click reactions, multicomponent couplings, and oxidation reactions.

1. Introduction

In contemporary organic synthesis, a central objective is to develop efficient catalytic methods that advance drug discovery, facilitate fine chemical synthesis, and support the sustainable production of industrial building blocks.[1–3] Catalysts with precisely defined multiple active sites, coupled with recyclability, offer significant advantages in terms of cost-effectiveness and environmental sustainability.[1,4,5] Due to their larger surface area and complex electronic structures, metal nanoparticles (MNPs) may demonstrate superior catalytic performance, exhibiting enhanced activity and selectivity compared to traditional homogenous metal catalyst.[1,4,6,7]

Nanoparticle systems, however, present significant challenges in the design and targeted synthesis, with surface-active sites that are difficult to customize. The exact bonding details of surface molecules often remain unclear due to the lack of detailed structural characterization.[7–9] As a result, there is a need to develop new catalysts that combine high atom utilization to enhance catalytic activity, with well-defined structures that enable detailed

KAUST Catalysis Center (KCC), King Abdullah University of Science and Technology (KAUST), Thuwal 23955-6900, Saudi Arabia. E-mail: magnus.rueping@kaust.edu.sa
† A. S. and K. M. contributed equally to this work.

mechanistic understanding. Achieving this balance is both highly desirable and inherently challenging.

In this context, metal nanoclusters (NCs) represent a unique class of nanomaterials. These clusters consist of a precise number of metal atoms stabilized by a specific number of ligands, resulting in well-defined, accessible structures.[8–10] NCs are typically represented as $[M_m(L)_n]^q$ (where m, n, and q correspond to the total number of metal atoms, ligands, and charge state, respectively).[10]

The ultra-small size of these clusters (<3 nm) provides a larger specific surface area and enhances catalytic activity.[8,9,11] Ligand-protected, atomically precise, high-purity nanoclusters (NCs) can be synthesized *via* wet chemical methods.[8] The properties of these clusters can be finely tuned by adjusting the number of metal atoms and the structure of the ligands, with even a single metal atom substitution significantly impacting the cluster's characteristics.[9–12] It is widely recognized that the size of the clusters can vary substantially depending on the specific reaction conditions and the initial concentrations of the reactants.[12] These size variations, in turn, lead to changes in the physicochemical properties of the clusters.[10] Quantum confinement effects are a key factor in this phenomenon, causing the transformation of continuous conduction and valence bands into discrete energy levels, particularly in clusters with dimensions smaller than 3 nm.[9,10,12] As a result, nanoclusters (NCs) with precisely defined compositions can

exhibit distinctive electronic transitions in the UV-vis spectrum, which are dependent on the size of the cluster's core.[13] The UV-vis absorption spectrum serves as a unique optical fingerprint, enabling both qualitative and quantitative analysis of a specific cluster. Notably, recent advancements in this field highlight the potential of these nanostructures as promising materials for a wide range of applications. A such NCs recently appeared as new catalysts for organic reactions including oxidations, reductions, C–C cross-couplings, A^3-couplings, and others.[9,14–19]

Despite their efficiency, a significant drawback of most nanoclusters is that they are composed of noble metals, which are expensive and scarce, thereby limiting their sustainable applicability.[9] Due to their abundance in the Earth's crust, cost-effectiveness, versatile ligand chemistry, and adjustable oxidation states, copper nanoclusters (CuNCs) have emerged as promising and sustainable catalysts for various bond-forming reactions. The catalytic applications of CuNCs have initially been relatively limited for specific reactions (*e.g.*, Click reactions, hydrogenations, and other catalytic processes processes)[15,20–27] primarily due to the insufficient availability and stability. However, recent advancements in synthesis have enabled the successful crystallization of a significant number of stable core–shell CuNCs.[22,28–30] In 2019 the Bakr research group reported the crystal structure of an atomically precise thiol-protected high-nuclearity core–shell **Cu$_{61}$** NC, [Cu$_{61}$(S^{t}Bu)$_{26}$S$_6$Cl$_6$H$_{14}$] that can be synthesized in large quantities following a simple synthetic procedure.[31]

The broad-range absorption in the visible light region, coupled with the richer photoluminescence properties (longer lifetimes) and well-defined structure of high-nuclearity core–shell CuNCs,[13,31–37] has inspired organic chemists to explore the catalytic activities of these materials in photoredox reactions.

This feature article provides an overview of the photocatalytic capabilities of copper-based nanoclusters for organic bond formations. Additionally, it outlines prospective directions for catalytic applications based on their precisely determined single-crystal and surface structures (see Fig. 1).


Fig. 1 Photoredox copper nanoclusters catalyzed organic bond-forming reactions.

2. Cross-coupling reactions

Cross-coupling reactions are among the most important processes for constructing complex organic molecules.[38] In this article, we summarize the C–N and C–C cross-couplings catalyzed by atomically precise Cu-based nanoclusters under photo-induced conditions.

2.1. C–N amination of aryl chlorides

In synthetic chemistry, the C–N arylation with nitrogen nucleophiles is a fundamentally significant reaction, widely utilized across various fields including agro- and pharmaceutical chemistry and the development of organic functional materials.[38–41]

Given the importance, numerous robust methodologies have been developed for constructing C–N bonds, including Ullmann–Goldberg couplings,[42–44] Buchwald–Hartwig aminations,[38] and Chan–Evans–Lam aminations.[45] Although copper has been employed as an abundant and inexpensive catalyst in Ullmann–Goldberg coupling, this process typically requires high reaction temperatures and activated electrophiles (*e.g.*, aryl bromides/iodides). In response the groups of Buchwald,[46,47] Taillefer,[44] and Ma[43,48,49] developed copper catalysts with diamine-based ligands to broaden the substrate scope for C–N coupling reactions, yet high temperatures were still necessary.[42–44] Fu and Peter's research group reported ultraviolet (UV) light-activated copper-catalyzed Ullmann C–N arylations of heteroatom nucleophiles.[50–53] Notably, with a judicious choice of ligand, it became possible to conduct copper-catalyzed C–N cross-couplings under visible light rather than traditional UV light.[54–58] More recently, hybrid Cu$_2$O nanocrystals have been employed for C–N cross-couplings *via* a photo-induced process.[59,60] However, while these are considered heterogeneous catalysts, the reaction mechanism remains poorly understood,[9] and their use has been limited to aryl iodides/bromide substrates.

As a result, there is a need to develop more effective and precisely structured catalysts for C–N cross-coupling reactions, particularly for the activation of cost-effective aryl chloride coupling agents. Additionally, a comprehensive understanding of catalytic mechanisms and the correlations between catalyst structure and properties would be necessary for advancing more efficient C–N bond forming reactions. Therefore, atomically precise copper nanocluster represents an optimal candidate for catalyzing C–N bond-forming reactions.

In 2022, our research group, in collaboration with the Bakr lab, made a pioneering discovery by demonstrating that the thiol-protected core–shell copper nanocluster [Cu$_{61}$(S^{t}Bu)$_{26}$S$_6$Cl$_6$H$_{14}$] (**Cu$_{61}$**) is an effective photocatalyst for the *N*-arylation of heterocyclic nucleophiles with unactivated aryl chlorides at room temperature (Fig. 2).[61]

The initial study established that the combination of **Cu$_{61}$**, a base, and visible light is essential for achieving the desired C–N coupling reaction, with yields reaching up to 88%. It was demonstrated that inorganic Cu salts (such as CuCl or CuCl$_2$) are less efficient, primarily due to their ineffectiveness to act as photocatalysts in the visible light region as compared to the **Cu$_{61}$** cluster catalyzed reaction.[51,53,54,57]
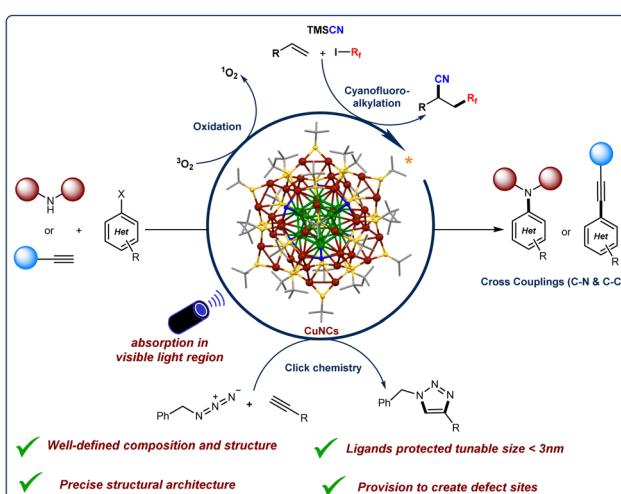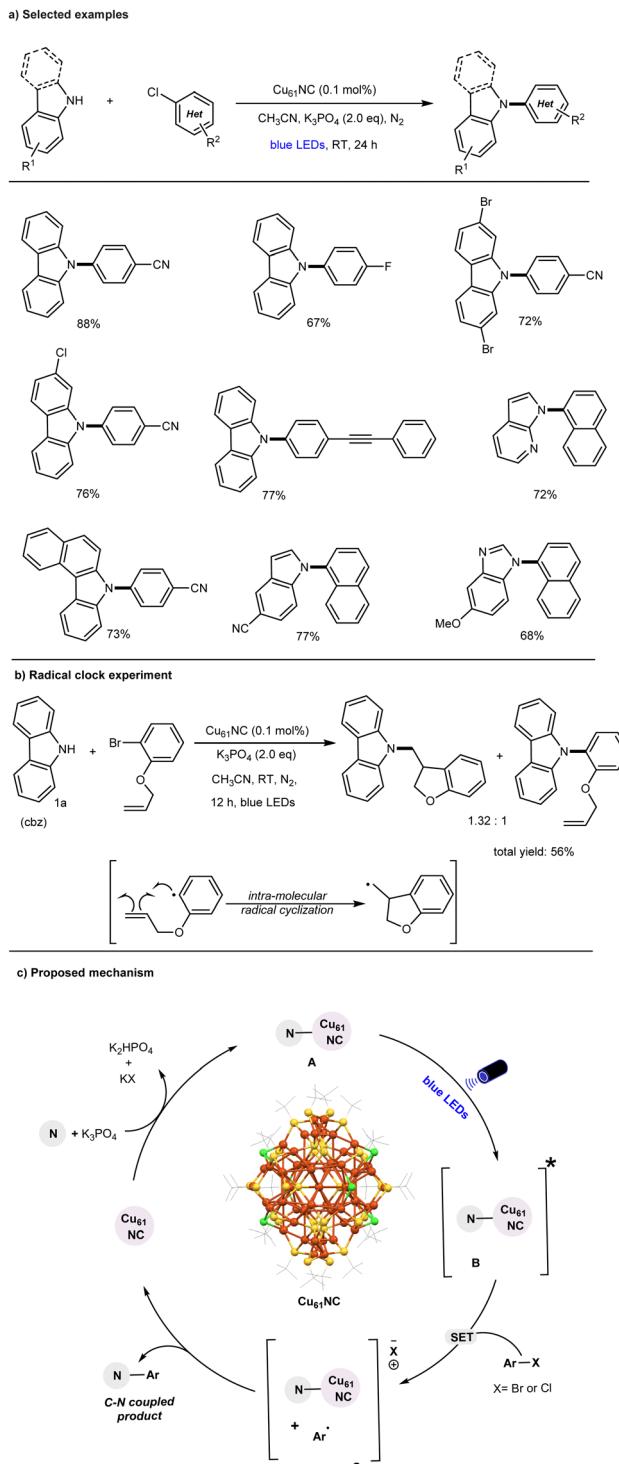
Fig. 2 Visible-light activated **Cu₆₁** NC catalyzed C–N amination of aryl chlorides.

The C–N bond formation catalyzed by the cluster exhibits a broad substrate scope, including typically unreactive aryl(hetero)-chlorides. Additionally, various heterocyclic N-nucleophiles were found to be compatible reaction partners, as illustrated in Fig. 2a Notably, this cluster-based approach marks a significant improvement over previously reported thermal copper-catalyzed

aryl chloride amination methods.[43,62–65] The **Cu₆₁** catalysis can be performed under mild reaction conditions (*i.e.*, room temperature) and accommodates a broad range of substrates, making it suitable for widespread application. Mechanistic control experiments, including radical clock experiments (Fig. 2b), competitive reactions, and radical trapping experiments, along with detailed spectroscopic studies, suggest that a facile single-electron transfer (SET) mechanism is operative in the CuNC-catalyzed C–N bond formation of aryl chlorides, in contrast to the traditional two-electron process.

The proposed mechanism is illustrated in Fig. 2c. The *in situ*-formed **Cu₆₁** NC-amine complex (**A**) is promoted to its photoexcited state (**B**) upon blue-light irradiation. In this excited state, the cluster complex (**B**) undergoes a facile single-electron transfer (SET) process with aryl chlorides, generating an aryl radical and an intermediate oxidized **Cu₆₁** NC–Nu complex (**C**). The highly reactive aryl radical subsequently undergoes a radical attack on the surface of complex **C**, leading to the C–N arylation product through either a radical-radical coupling pathway or a reductive elimination step. Overall, this successful transformation highlights the potential of CuNCs as emerging photocatalysts for challenging organic bond-forming reactions and provides valuable insights into the role of their core–shell structural architecture under photoinduced conditions.

2.2. Sonogashira C–C cross-coupling

The Sonogashira reaction is widely recognized as a straightforward and efficient method for the synthesis of alkyne derivatives. It is commonly used in the production of natural products, medicinal chemistry, pharmaceutical manufacturing, and the development of functional materials.[66–68] Given the importance, an array of catalytic methods have been established for such cross-couplings, including (a) conventional Pd/Cu-catalytic methods with amine bases,[69,70] (b) Cu-free Pd-catalytic methods,[71–73] (c) Pd-free Fe-, Ni-catalysis,[74–76] (d) Pd-free, copper catalysis,[77–80] and (e) MNPs (including Pd- or Cu-NPs catalysis).[81–85] Recently, photocatalytic Cu nanoparticles (Cu-NPs) have also been shown to catalyze Sonogashira couplings under a CO_2 atmosphere.[86] The required CO_2 promotes the formation of an active catalyst surface-bound Cu(ɪ)-phenylacetylide complex *via* the formation of inorganic carbonate ($CuCO_3$), with a working principle similar to that of conventional Cu catalysts.[78] However, modeling nanoparticle systems remains challenging due to their complex atomic surface structures, and the suitability of these ambiguous structures for catalytic applications may be subject to scrutiny.[9] In previously reported copper-catalyzed Sonogashira reactions, significant to high amounts of Glaser homocoupling by-products are often formed.[79,80,85,86] Mechanistically, the polymeric nature of the copper-acetylide intermediate plays a key role in the formation of Glaser homocoupling by-products during the copper-catalyzed Sonogashira reaction.[87–89]

Addressing these challenges, the development of a novel copper-catalyzed system with enhanced selectivity for C–C coupled products, while minimizing the formation of undesired homocoupled alkyne by-products, remains a key objective. In this context, the Rueping and Bakr groups recently highlighted

a) Selected examples

b) Proposed mechanism
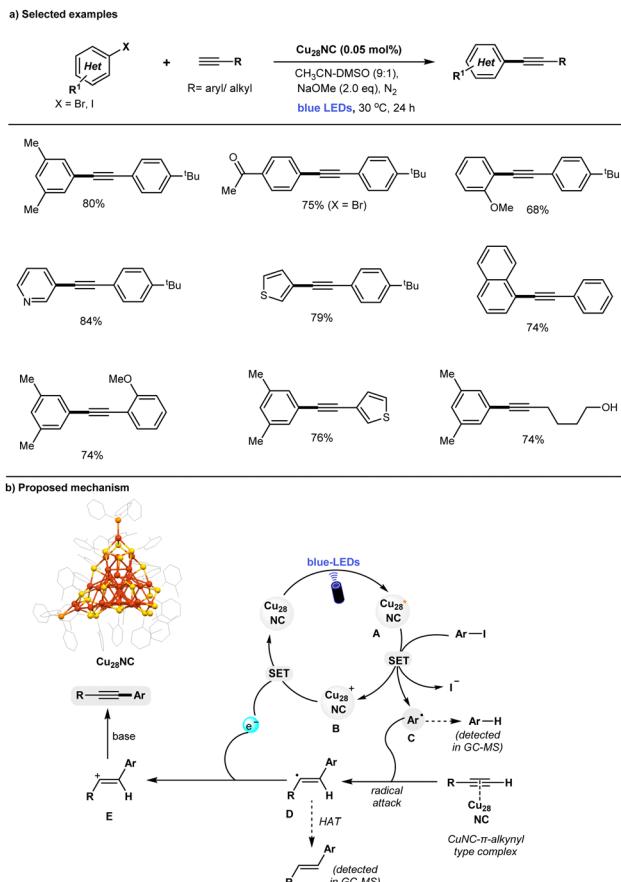
Fig. 3 Defects **Cu$_{28}$** NC catalyzed Sonogashira C–C coupling reactions under photoinduced conditions.

the unique characteristics of $[Cu_{28}H_{10}(C_7H_7S)_{18}(TPP)_3]$ (**Cu$_{28}$**) nanoclusters (NCs), which demonstrate high selectivity as catalysts for Sonogashira C–C coupling reactions under visible light irradiation (Fig. 3).[90] Control experiments have revealed that light, base, and **Cu$_{28}$** are essential for the observed reaction. The defective **Cu$_{28}$** nanocluster is compatible with a broad range of substrates, including various aryl iodides and terminal alkynes, delivering Sonogashira C–C coupled products in good to excellent yields (up to 84%). Notably, the presence of defects in **Cu$_{28}$** play a crucial role in achieving high selectivity in the Sonogashira C–C coupling reaction, effectively preventing the problematic formation of undesired homo-coupling alkyne byproducts. In contrast, traditional copper catalytic systems, such as CuCl, $Cu(CH_3CN)_4BF_4$, or CuNPs, exhibit lower yields and inferior selectivity in comparison. Additionally, the study explored a larger cluster family, **Cu$_{61}$** NCs, in the same reaction. However, these clusters proved to be less efficient compared to the defective **Cu$_{28}$** catalyst. A series of control experiments demonstrated that the defective **Cu$_{28}$** outperformed traditional copper catalysts. Notably, after the completion of the reaction, the recovered **Cu$_{28}$** catalyst remained unchanged, highlighting its remarkable stability. A set of mechanistic control experiments support the formation of Ar-radical *via* SET process between the photoexcited state of **Cu$_{28}$** and aryl iodides. The proposed

mechanism is shown in Fig. 3b. Upon blue-light irradiation of ground-state **Cu$_{28}$**, its long-lived photoexcited state is generated that participates in a SET process with aryl iodides (E_{red} = −1.7 to −2.3 V *vs.* SCE)[91,92] to generate the Ar-radical **C** and oxidized form of **Cu$_{28}$** **B**. The highly reactive Ar-radical attacks the C–C triple bond of the alkynes to produce vinylic-type carbon-centered radical intermediate **D**, and a subsequent back SET process to **Cu$_{28}^+$** (**B**) regenerates the ground state **Cu$_{28}$** photocatalyst. Finally, base-promoted deprotonation of vinyl cation **E** leads to form desired Sonogashira C–C coupled products with high selectivity. In contrast to conventional inorganic copper-catalyst[79,85,86] and Cu(I)-acetylide cluster,[87,89] **Cu$_{28}$** may not form a CuNC-phenylacetylide-intermediate (supported by various control experiments). Thus, the defective **Cu$_{28}$** can act as a putative photocatalyst that involves the SET process with aryl iodides to generate the Ar-radical and subsequently attacks the C–C triple bond, thus preventing the formation of the homocoupling byproduct.

Recently, the Negishi group successfully synthesized the luminescent, hydride-free $[Cu_7(SC_5H_9)_7(PPh_3)_3]$ (**Cu$_7$** NC) and explored its catalytic application in the Sonogashira cross-coupling reaction under photoinduced conditions (Fig. 4).[93] Control experiments revealed that the exclusion of **Cu$_7$** NC, light, or base resulted in no reaction. Notably, the **Cu$_7$** NC catalyst can be recovered, as confirmed by UV-vis absorption spectra, and remains intact even after 10 reaction cycles.

Under optimized reaction conditions, a broad range of aryl halides (X = I, Br) were successfully coupled with various aryl

a) Selected example

b) Proposed mechanism
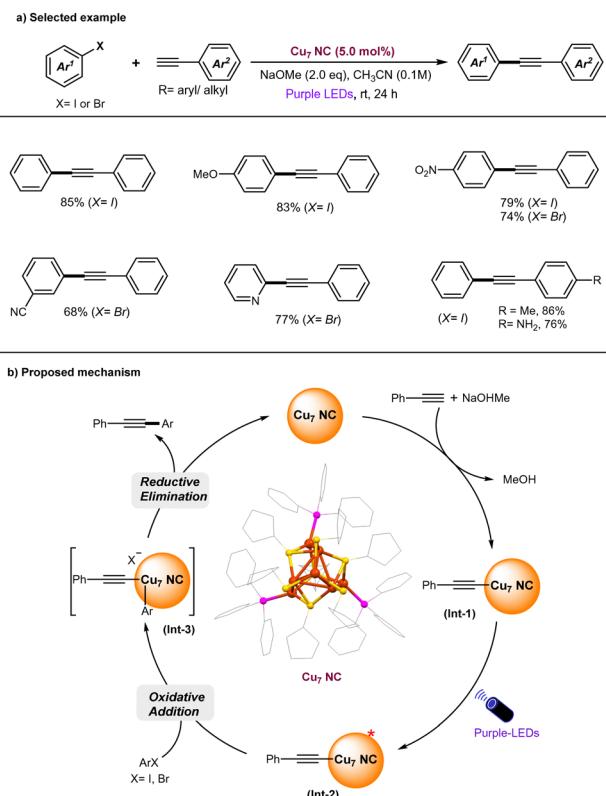
Fig. 4 Luminescent **Cu$_7$** NC catalyzed Sonogashira C–C coupling reactions under photoinduced conditions.

alkynes, yielding the C–C coupled Sonogashira products in excellent yields and with high selectivity (Fig. 4a). Based on experimental results, supported by theoretical studies, the reaction mechanism is proposed to follow a polar pathway rather than a radical-based mechanism. The proposed mechanism is illustrated in Fig. 4b. Initially, Cu_7 nanoclusters (NCs) interact with phenylacetylene in the presence of a base, forming a Cu-phenylacetylide intermediate (**Int-1**). Upon photoexcitation, the ground-state **Int-I** is excited to generate a photoexcited state (**Int-2**), which subsequently undergoes oxidative addition with aryl halides, leading to the formation of **Int-III**. Finally, a reductive elimination step from **Int-III** results in the formation of the C–C coupled products and the regeneration of the original Cu_7 NCs. It was identified that in the current Cu_7 NC-catalyzed Sonogashira C–C coupling reaction, the oxidative addition step is rate-determining, closely aligning with the mechanism observed in thermally mediated Cu-catalyzed Sonogashira reactions[78,80] Alternatively, the photoexcited state of **Int-2** may undergo a SET process with ArX to generate an aryl radical and the oxidized form of **Int-2**. The highly reactive aryl radical is set to attack the oxidized form of **Int-2** to deliver desired C–C coupled products and allows re-generation of original Cu_7 NC. Indeed, inorganic copper(I) phenylacetylides were shown to undergo facile intersystem crossing,[94–98] therefore, a radical process cannot be ruled out.

3. Click reactions

The copper(I)-catalyzed [3 + 2] azide–alkyne cycloaddition (CuAAC) stands out as a versatile reaction in the field of "click chemistry for the construction of 1,4-triazoles.[99–102] In 2002, the research group of Meldal[103] and Sharpless[104] disclosed CuAAC reactions, which have had a wide variety of applications in synthetic chemistry,[105–107] polymers and material science,[108,109] and bio-conjugation chemistry.[110–112]

The significance of click chemistry was underscored by the Nobel Prize in Chemistry awarded to Bertozzi, Meldal, and Sharpless.[113] Traditionally, the click reaction is catalyzed by air-sensitive, unstable Cu^I complexes or by stable Cu^{II} salts in the presence of a chemical reducing agent, such as sodium ascorbate, under thermally mediated conditions.[114,115] More recently, a photo-click reaction has been reported,[116–118] where the active Cu^I catalyst is generated *in situ via* the photoreduction of a stable Cu^{II} complex. However, light-induced click reactions offer greater benefits compared to traditional click reactions performed in the absence of light (dark conditions). For instance, photo-click reactions can be triggered at precise moments and locations, making them a potent tool for chemical synthesis, bio-orthogonal conjugation, and customized material production.[117,119]

Hence, there is a strong desire for the creation of a novel and precisely structured copper-based photocatalyst for click reactions. Recently, atomically precise Cu-nanoclusters *e.g.*, $(Cu_{20}(PhCC)_{12}(OAc)_6)$ have been shown as a modular catalyst for CuAAC reaction,[22,120,121] however, this catalytic system is

still operative under thermal conditions rather than a photoinduced process. In the most recent developments, the Rueping and Bakr groups collaboratively published findings on the production of atomically precise copper hydride nanoclusters, $[Cu_{58}H_{20}PET_{36}(PPh_3)_4]^{2+}$ (Cu_{58}; PET: phenylethanethiolate; PPh_3: triphenylphosphine).[122] One surface copper atom of Cu_{58} is chemically removed during the recrystallization process, which results in a defective analogous nanocluster namely, $[Cu_{57}H_{20}PET_{36}(PPh_3)_4]^+$ (Cu_{57}) (Fig. 5a). Indeed, the single-atom manipulation on stable copper hydride nanocluster (Cu_{58}) could drastically alter their reactivity of the nanocluster. Catalytic explorations revealed that the defective Cu_{57} nanocluster acted as an efficient photocatalyst, delivering the click product in 97% yield, whereas the parent copper nanocluster (Cu_{58}) produced only 77% yield after 1.5 hours of visible-light irradiation (Fig. 5b). Cu_{57} and Cu_{58} were found to exhibit good stability during photoirradiation under blue LEDs in acetonitrile. Control experiments, such as conducting the reaction in the dark or using conventional copper catalysts (*e.g.*, CuCl), showed significantly lower efficiency. Mechanistic control studies revealed that this photocatalytic click reaction follows a radical pathway, as opposed to the traditional two-electron process. The superior catalytic performance of Cu_{57} compared to Cu_{58} is attributed to the creation of an active catalytic site in Cu_{57} due to the removal of a surface copper atom. This insight could inspire further exploration of single-atom chemistry in metal nanoclusters and enable researchers to fine-tune their properties for catalytic applications in organic reactions.

In relation to Cu-cluster-catalyzed photo-click reactions, Jiang and co-workers recently synthesized the dimeric anionic supramolecular cluster $[Cu_8I_{14}]^{6-}$ (**HUBU-1**), which has been demonstrated to be an effective photocatalyst for both the oxidative coupling of benzylamine and the azide–alkyne cycloaddition reaction.[120]

4. Multicomponent coupling

Recently, He and co-workers synthesized and characterized $[Cu_{40}H_{17}(2,4\text{-}DMBT)_{24}](PPh_4)$ (denoted as Cu_{40}-H NC) which displays enhanced photophysical properties along with excellent air and moisture stability.[123] The photoexcitation of this
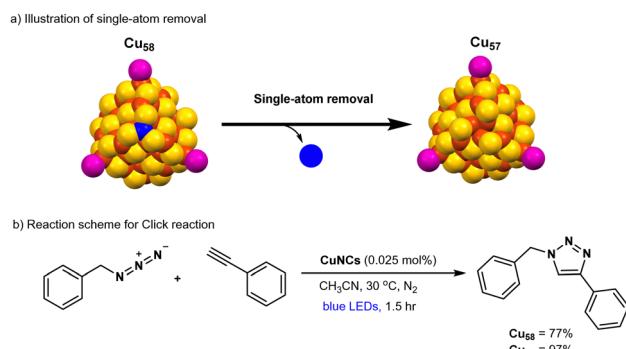

Fig. 5 Isostructural Cu_{57} NC & Cu_{58} NC catalyzed Click reactions.

structurally well-defined anionic **Cu₄₀**-H NC exhibits remarkable NIR-II (1000–1700 nm) emissive properties.

Moreover, the **Cu₄₀**-H NC photocatalyst demonstrated high efficiency in a three-component coupling reaction involving alkenes, fluoroalkyl iodides, and trimethylsilyl cyanide, yielding the desired coupled products in excellent yields with high turnover numbers (TON) (Fig. 6a). Based on a series of control experiments, the proposed reaction mechanism is illustrated in Fig. 6b. Upon irradiation with blue LEDs, the anionic **Cu₄₀**-H NC is excited to its photoexcited state (**Int-A**), followed by a single electron transfer (SET) process with fluoroalkyl iodides, generating a reactive alkyl radical (R•) and a cluster intermediate (**Int-B**). The highly reactive alkyl radical readily attacks the terminal alkene, generating a secondary alkyl radical. In the next step, cluster intermediate B reacts with TMSCN to form an anionic cyanide-ligated cluster intermediate (**Int-C**), which subsequently reacts with the secondary alkyl radical to afford the C–C coupling product and regenerate the original anionic **Cu₄₀**-H NC. Overall, the NIR-II emissive anionic **Cu₄₀**-H NC has been demonstrated as a highly efficient photoredox catalyst for the cyanofluoroalkylation of alkenes with a broad range of substrates under blue-LED irradiation.
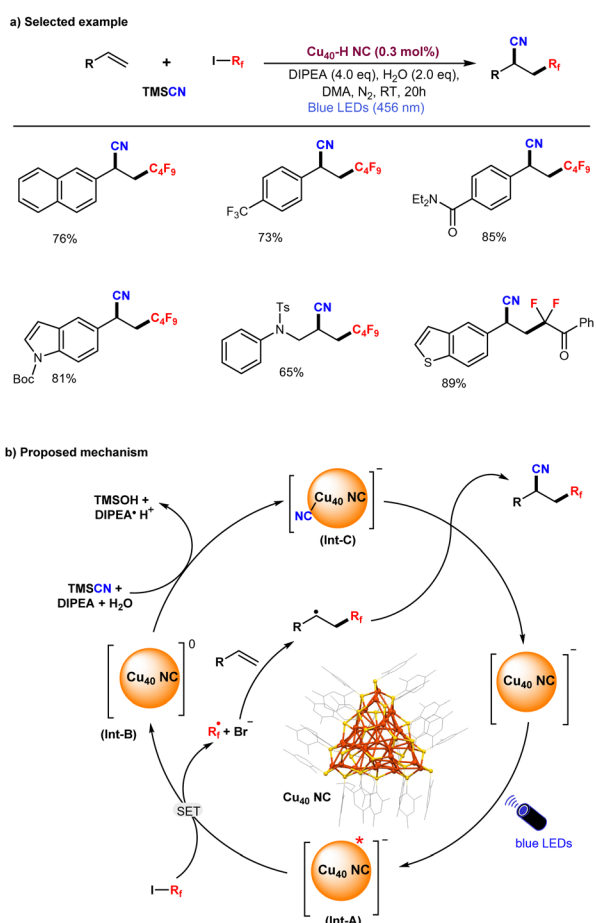
5. Photooxidation by singlet oxygen

Singlet oxygen ($^1O_2$) is known to be a key reactive oxygen species (ROS) and plays an indispensable role in photocatalytic organic reactions (*e.g.*, Ene reactions)[124] and photodynamic therapy.[125] Indeed, metal nanoclusters (MNCs) are shown as powerful photosensitizers for $^1O_2$-mediated photocatalytic organic reactions *via* an energy transfer process with molecular oxygen ($^3O_2$).[126] In this context, Zhang *et al.* recently reported the successful preparation of two quasi-structurally isomeric **Cu₁₃** NCs (denoted as **Cu₁₃a** and **Cu₁₃b**) and demonstrated their effectiveness in the photocatalytic oxidation of sulfides (Fig. 7a).[127] These isomeric structures of **Cu₁₃** nanoclusters are protected by CZ-PrAH (9-(prop-2-yn-1-yl)-9*H*-carbazole) and H₄TC4A (*p-tert*-butylthiacalix[4]arene) ligands. The formula of these NCs is [Cu₁₃Na(CZ-PrA)₆(TC4A)₂(CH₃OH)]·CH₃OH· CH₂-Cl₂·CH₃COCH₃ and [Cu₁₃Na₂(CZ-PrA)₆(TC4A)₂Cl(CH₃OH)₂]. The two **Cu₁₃** nanoclusters (NCs) exhibit structural similarities; however, the primary distinction lies in the attachment of a chloride anion to the metallic framework, influenced by solvent-induced effects during the crystallization process.

Upon photoexcitation, the chloride anion engages in a charge transfer process with the metal core, a process more efficient in the **Cu₁₃a** structure compared to **Cu₁₃b**. This charge transfer event significantly alters the electronic band structure of **Cu₁₃a**, leading to a higher production of singlet oxygen ($^1O_2$) rather than superoxide radical anion ($O_2^{•-}$), compared to **Cu₁₃b**. As a result, the **Cu₁₃a** structure demonstrates superior photocatalytic performance in the selective oxidation of dimethyl sulfide, with selectivity exceeding 99.9%. The series of trapping experiments such as DMPO (5,5-dimethyl-1-pyrroline-*N*-oxide) and TEMPO (2,2,6,6-tetramethylpiperidine-*N*-oxyl), and DFT study indicates that **Cu₁₃a** is an effective for selective photocatalytic oxidation of dimethyl sulfide. Overall, this work reveals that the attachment of chloride ions to the surface of Cu nanoclusters (CuNCs) can create more active sites to produce

Fig. 6 NIR-II emissive anionic **Cu₄₀** NC photoredox catalyzed cyanofluoroalkylation of alkenes.
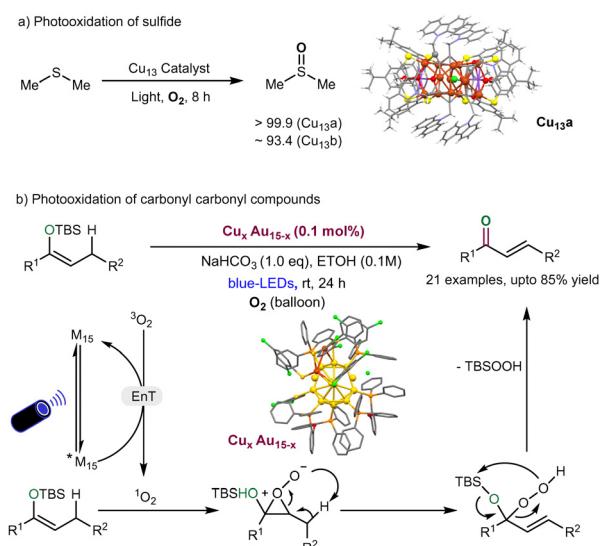
Fig. 7 (a) Quasi-structurally isomeric **Cu₁₃** NCs catalysed photocatalytic sulfoxidation of sulfides. (b) Photo-oxidation of carbonyl compound derivatives by Cu$_x$Au$_{15-x}$ NCs.
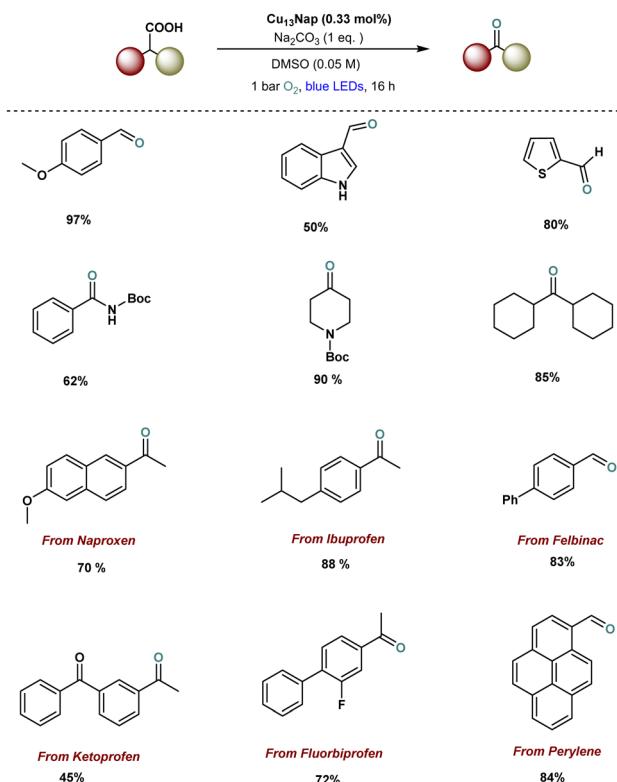
Fig. 8 Ligand-engineered **Cu$_{13}$** NCs catalysed photocatalytic decarboxylative oxidation reaction.

singlet oxygen ($^1O_2$), specifically targeting selective photocatalytic oxidation reactions. This discovery significantly expands the potential for various chemical reactions, opening new possibilities for advanced catalytic applications. Very recently, Zhu and coworkers[128] synthesized and characterized the homogold Au$_{15}$ and Au–alloy clusters such as AgAu$_{15}$ and Cu$_x$Au$_{15-x}$, trimetallic Ag$_x$Cu$_y$Au$_{15-x-y}$, and tetramettalic Pt$_1$Ag$_x$Cu$_y$Au$_{15-x-y}$. In the evaluation of the photophysical properties of Au–alloy nanoclusters, the phosphorescence of Cu$_x$Au$_{15-x}$ nanocluster displayed efficient singlet oxygen generation for photooxidation of carbonyl compounds to produce α,β-unsaturated ketones under blue-LEDs irradiation (Fig. 7b). The reaction pathway follows the energy transfer process and is followed by singlet oxygen generation, enabling photooxidation of carbonyl derivatives.

Recently, our group successfully designed ligand-engineered, atomically precise copper nanoclusters, including Cu$_{13}$(Nap)$_3$-(PPh$_3$)$_7$H$_{10}$ (Cu$_{13}$Nap) and Cu$_{13}$(DCBT)$_3$(PPh$_3$)$_7$H$_{10}$ (Cu$_{13}$DCBT) and demonstrated their photocatalytic application in decarboxylative oxidation reactions (Fig. 8).[129] Notably, Cu$_{13}$Nap, stabilized by naphthalene thiolate ligands, achieved a remarkable 90% yield in the decarboxylative oxidation, significantly outperforming the isostructural Cu$_{13}$(DCBT)$_3$(PPh$_3$)$_7$H$_{10}$ (Cu$_{13}$DCBT), which gave a 28% yield. This enhanced performance is attributed to ligand engineering, which modulates the electronic structure, enhances visible light absorption, and facilitates energy transfer mechanisms during the reaction. In contrast to conventional decarboxylative oxidation reactions, which typically follow a single-electron transfer (SET) pathway, the mechanism here is primarily driven by energy transfer, as confirmed by density functional theory (DFT) calculations and experimental evidence. This study highlights the profound impact of ligand modification on copper nanoclusters (Cu NCs), opening new avenues for developing more sustainable and efficient photocatalytic systems. Furthermore, the catalytic system exhibits broad substrate compatibility and excellent tolerance for various functional groups. Particularly, the successful decarboxylation of fully aliphatic acids and the late-stage modification of drug molecules, as shown in examples 11–17, underscores the potential of this catalyst to address key challenges in drug discovery.

6. Conclusions and outlook

In light of the growing applications of modern photochemistry in drug discovery and biological synthesis, the need for the development and refinement of highly efficient catalysts has become increasingly important. This review highlights the potential of atomically precise copper nanoclusters (CuNCs) as innovative photocatalysts for a diverse range of bond-forming reactions, including C–C and C–N couplings, copper-catalyzed azide–alkyne cycloaddition (CuAAC), multicomponent couplings, and oxidation reactions. These findings suggest that CuNCs can play a transformative role in catalysis, extending beyond their conventional use as copper-based catalysts, and offering new possibilities for advancements in chemical synthesis. Unlike noble metal nanoclusters, the synthesis of copper nanoclusters (CuNCs) is significantly more challenging due to their lower half-reduction potential, which raises concerns about their stability in catalytic applications. However, recent studies have shown that the use of carefully selected thiol and phosphorus-containing ligands enables the successful synthesis of stable CuNCs in larger quantities, making them suitable for catalyzing organic reactions. Despite this progress, examining the structural stability of CuNCs when subjected to photoinduced conditions during catalytic reactions is important. To date the structures of **Cu$_7$**, **Cu$_{28}$**, **Cu$_{58}$**, and **Cu$_{57}$** have shown to remain stable under blue LED irradiation.

In comparison to homogeneous systems, heterogeneous materials are more appropriate for industrial applications due to their stability and recyclability. Therefore, there is a strong demand to develop stable, recyclable and precisely structured CuNCs. Furthermore, the development of chiral CuNCs for enantioselective reactions presents a promising area of interest. However, this endeavour is particularly challenging, as the chiral ligands must fulfil dual roles: stabilizing the clusters while also inducing high enantioselectivity.

In conclusion, the exploration of Cu-based nanocluster (CuNC) catalysis offers promising opportunities for advancing unique bond-forming reactions. We hope that this review will inspire further research into Cu-based cluster catalysis, leading to novel approaches in organic synthesis and expanding the role of CuNCs in catalysis.

Conflicts of interest

The authors declare no competing financial interest.

Notes and references

1 L. L. Chng, N. Erathodiyil and J. Y. Ying, *Acc. Chem. Res.*, 2013, **46**, 1825–1837.
2 I. Ghosh, N. Shlapakov, T. A. Karl, J. Düker, M. Nikitin, J. V. Burykina, V. P. Ananikov and B. König, *Nature*, 2023, **619**, 87–93.
3 C.-J. Li and B. M. Trost, *Proc. Natl. Acad. Sci. U. S. A.*, 2008, **105**, 13197–13202.
4 N. K. Ojha, G. V. Zyryanov, A. Majee, V. N. Charushin, O. N. Chupakhin and S. Santra, *Coord. Chem. Rev.*, 2017, **353**, 1–57.
5 B. Trost, *Science*, 1991, **254**, 1471–1477.
6 L. Liu and A. Corma, *Chem. Rev.*, 2018, **118**, 4981–5079.
7 M. B. Gawande, A. Goswami, F.-X. Felpin, T. Asefa, X. Huang, R. Silva, X. Zou, R. Zboril and R. S. Varma, *Chem. Rev.*, 2016, **116**, 3722–3811.
8 I. Chakraborty and T. Pradeep, *Chem. Rev.*, 2017, **117**, 8208–8271.
9 Y. Du, H. Sheng, D. Astruc and M. Zhu, *Chem. Rev.*, 2020, **120**, 526–622.
10 R. Jin, C. Zeng, M. Zhou and Y. Chen, *Chem. Rev.*, 2016, **116**, 10346–10413.
11 R. Jin, G. Li, S. Sharma, Y. Li and X. Du, *Chem. Rev.*, 2021, **121**, 567–648.
12 A. Ghosh, O. F. Mohammed and O. M. Bakr, *Acc. Chem. Res.*, 2018, **51**, 3094–3103.
13 R.-W. Huang, J. Yin, C. Dong, A. Ghosh, M. J. Alhilaly, X. Dong, M. N. Hedhili, E. Abou-Hamad, B. Alamer, S. Nematulloev, Y. Han, O. F. Mohammed and O. M. Bakr, *J. Am. Chem. Soc.*, 2020, **142**, 8696–8705.
14 T. Higaki, Y. Li, S. Zhao, Q. Li, S. Li, X.-S. Du, S. Yang, J. Chai and R. Jin, *Angew. Chem., Int. Ed.*, 2019, **58**, 8291–8302.
15 C. Sun, N. Mammen, S. Kaappa, P. Yuan, G. Deng, C. Zhao, J. Yan, S. Malola, K. Honkala, H. Häkkinen, B. K. Teo and N. Zheng, *ACS Nano*, 2019, **13**, 5975–5986.
16 J. Hu, Y.-M. Li, B. Zhang, X. Kang and M. Zhu, *Inorg. Chem. Front.*, 2024, **11**, 4974–5003.
17 J. Wang, J. Cai, K.-X. Ren, L. Liu, S.-J. Zheng, Z.-Y. Wang and S.-Q. Zang, *Sci. Adv.*, 2024, **10**, eadn7556.
18 H. Guo, Y. Chen, Y.-Z. Han, Q. Wu, L. Wang, Q. Xu, R. Huo, X. Gong, J. Sun, Q. Tang and H. Shen, *Chem. Mater.*, 2024, **36**, 7243–7251.
19 M. S. Mathew, G. Krishnan, A. A. Mathews, K. Sunil, L. Mathew, R. Antoine and S. Thomas, *Nanomaterials*, 2023, **13**, 1874.
20 B. Mondal, K. Basu, R. Jana, P. Mondal, B. Hansda, A. Datta and A. Banerjee, *ACS Appl. Nano Mater.*, 2022, **5**, 7932–7943.
21 S. Lee, M. S. Bootharaju, G. Deng, S. Malola, W. Baek, H. Häkkinen, N. Zheng and T. Hyeon, *J. Am. Chem. Soc.*, 2020, **142**, 13974–13981.
22 A. W. Cook, Z. R. Jones, G. Wu, S. L. Scott and T. W. Hayton, *J. Am. Chem. Soc.*, 2018, **140**, 394–400.
23 G. Yang, Y. Xie, Y. Wang, Y. Tang, L. L. Chng, F. Jiang, F. Du, X. Zhou, J. Y. Ying and X. Yuan, *Nano Res.*, 2023, **16**, 1748–1754.
24 C.-Y. Liu, T.-Y. Liu, Z.-J. Guan, S. Wang, Y.-Y. Dong, F. Hu, D.-E. Jiang and Q.-M. Wang, *CCS Chem.*, 2024, **6**, 1581–1590.
25 P. Kumar and M. Nemiwal, *Chem. – Asian J.*, 2024, **19**, e202400062.
26 B. Yan, X. You, X. Tang, J. Sun, Q. Xu, L. Wang, Z.-J. Guan, F. Li and H. Shen, *Chem. Mater.*, 2024, **36**, 1004–1012.
27 L. Dong, L. Yu, X. Sun, X. Tang, X. You, J. Tang, Z.-A. Nan, D. Cao, Y. Jia, S. Li, F. Li, S. Guo and H. Shen, *Inorg. Chem. Front.*, 2023, **10**, 5745–5751.
28 T.-A. D. Nguyen, Z. R. Jones, B. R. Goldsmith, W. R. Buratto, G. Wu, S. L. Scott and T. W. Hayton, *J. Am. Chem. Soc.*, 2015, **137**, 13319–13324.
29 T.-A. D. Nguyen, Z. R. Jones, D. F. Leto, G. Wu, S. L. Scott and T. W. Hayton, *Chem. Mater.*, 2016, **28**, 8385–8390.
30 P. Yuan, R. Chen, X. Zhang, F. Chen, J. Yan, C. Sun, D. Ou, J. Peng, S. Lin, Z. Tang, B. K. Teo, L.-S. Zheng and N. Zheng, *Angew. Chem., Int. Ed.*, 2019, **58**, 835–839.
31 A. Ghosh, R.-W. Huang, B. Alamer, E. Abou-Hamad, M. N. Hedhili, O. F. Mohammed and O. M. Bakr, *ACS Mater. Lett.*, 2019, **1**, 297–302.
32 C. Dong, R.-W. Huang, C. Chen, J. Chen, S. Nematulloev, X. Guo, A. Ghosh, B. Alamer, M. N. Hedhili, T. T. Isimjan, Y. Han, O. F. Mohammed and O. M. Bakr, *J. Am. Chem. Soc.*, 2021, **143**, 11026–11035.
33 S. Biswas, S. Das and Y. Negishi, *Nanoscale Horiz.*, 2023, **8**, 1509–1522.
34 N. Li, B. Li, H. Murugesan, A. Sagadevan and M. Rueping, *ACS Catal.*, 2024, 11974–11989, DOI: **10.1021/acscatal.4c03238**.
35 A. Ghosh, A. Sagadevan, K. Murugesan, S. A. F. Nastase, B. Maity, M. Bodiuzzaman, A. Shkurenko, M. N. Hedhili, J. Yin,

36 B. Alamer, A. Sagadevan, M. Bodiuzzaman, K. Murugesan, S. Alsharif, R.-W. Huang, A. Ghosh, M. H. Naveen, C. Dong, S. Nematulloev, J. Yin, A. Shkurenko, M. Abulikemu, X. Dong, Y. Han, M. Eddaoudi, M. Rueping and O. M. Bakr, *J. Am. Chem. Soc.*, 2024, **146**, 16295–16305.
37 A. Jana, S. Duary, A. Das, A. R. Kini, S. Acharya, J. Machacek, B. Pathak, T. Base and T. Pradeep, *Chem. Sci.*, 2024, **15**, 13741–13752, DOI: **10.1039/D4SC01566E**.
38 P. Ruiz-Castillo and S. L. Buchwald, *Chem. Rev.*, 2016, **116**, 12564–12649.
39 G. Ćirić-Marjanović, *Synth. Met.*, 2013, **177**, 1–47.
40 E. Vitaku, D. T. Smith and J. T. Njardarson, *J. Med. Chem.*, 2014, **57**, 10257–10274.
41 H.-J. Knölker, *The alkaloids: chemistry and biology*, Academic Press, 2011, vol. 70.
42 C. Sambiagio, S. P. Marsden, A. J. Blacker and P. C. McGowan, *Chem. Soc. Rev.*, 2014, **43**, 3525–3550.
43 S. Bhunia, G. G. Pawar, S. V. Kumar, Y. Jiang and D. Ma, *Angew. Chem., Int. Ed.*, 2017, **56**, 16136–16179.
44 F. Monnier and M. Taillefer, *Angew. Chem., Int. Ed.*, 2009, **48**, 6954–6971.
45 J. X. Qiao and P. Y. S. Lam, *Synthesis*, 2011, 829–856.
46 D. S. Surry and S. L. Buchwald, *Chem. Sci.*, 2010, **1**, 13–31.
47 S.-T. Kim, M. J. Strauss, A. Cabré and S. L. Buchwald, *J. Am. Chem. Soc.*, 2023, **145**, 6966–6975.
48 S. Bhunia, S. De and D. Ma, *Org. Lett.*, 2022, **24**, 1253–1257.
49 Q. Yang, Y. Zhao and D. Ma, *Org. Process Res. Dev.*, 2022, **26**, 1690–1750.
50 A. Hossain, A. Bhattacharyya and O. Reiser, *Science*, 2019, **364**, eaav9713.
51 S. E. Creutz, K. J. Lotito, G. C. Fu and J. C. Peters, *Science*, 2012, **338**, 647–651.
52 A. C. Bissember, R. J. Lundgren, S. E. Creutz, J. C. Peters and G. C. Fu, *Angew. Chem., Int. Ed.*, 2013, **52**, 5129–5133.
53 D. T. Ziegler, J. Choi, J. M. Muñoz-Molina, A. C. Bissember, J. C. Peters and G. C. Fu, *J. Am. Chem. Soc.*, 2013, **135**, 13107–13112.
54 Q. M. Kainz, C. D. Matier, A. Bartoszewicz, S. L. Zultanski, J. C. Peters and G. C. Fu, *Science*, 2016, **351**, 681–684.
55 C. D. Matier, J. Schwaben, J. C. Peters and G. C. Fu, *J. Am. Chem. Soc.*, 2017, **139**, 17707–17710.
56 C. Chen, J. C. Peters and G. C. Fu, *Nature*, 2021, **596**, 250–256.
57 J. M. Ahn, T. S. Ratani, K. I. Hannoun, G. C. Fu and J. C. Peters, *J. Am. Chem. Soc.*, 2017, **139**, 12716–12723.
58 H. Cho, H. Suematsu, P. H. Oyala, J. C. Peters and G. C. Fu, *J. Am. Chem. Soc.*, 2022, **144**, 4550–4558.
59 G. Singh, M. Kumar and V. Bhalla, *Green Chem.*, 2018, **20**, 5346–5357.
60 Z. Xu, W. Wang, Y. Xu, S. Song, J. Yu, W. Song, H. Xu, H. Fu and Z. Li, *ACS Catal.*, 2023, **13**, 13920–13930.
61 A. Sagadevan, A. Ghosh, P. Maity, O. F. Mohammed, O. M. Bakr and M. Rueping, *J. Am. Chem. Soc.*, 2022, **144**, 12052–12061.
62 W. Liu, J. Xu, X. Chen, F. Zhang, Z. Xu, D. Wang, Y. He, X. Xia, X. Zhang and Y. Liang, *Org. Lett.*, 2020, **22**, 7486–7490.
63 S. Xia, L. Gan, K. Wang, Z. Li and D. Ma, *J. Am. Chem. Soc.*, 2016, **138**, 13493–13496.
64 W. Zhou, M. Fan, J. Yin, Y. Jiang and D. Ma, *J. Am. Chem. Soc.*, 2015, **137**, 11942–11945.
65 Z. Chen and D. Ma, *Org. Lett.*, 2019, **21**, 6874–6878.
66 C. C. C. J. Seechurn, M. O. Kitching, T. J. Colacot and V. Snieckus, *Angew. Chem., Int. Ed.*, 2012, **51**, 5062–5085.
67 O. Mongin, L. Porrès, L. Moreaux, J. Mertz and M. Blanchard-Desce, *Org. Lett.*, 2002, **4**, 719–722.
68 I. Paterson, R. D. M. Davies and R. Marquez, *Angew. Chem., Int. Ed.*, 2001, **40**, 603–607.
69 K. Sonogashira, Y. Tohda and N. Hagihara, *Tetrahedron Lett.*, 1975, **16**, 4467–4470.
70 H. Doucet and J.-C. Hierso, *Angew. Chem., Int. Ed.*, 2007, **46**, 834–871.
71 K. C. Dissanayake, P. O. Ebukuyo, Y. J. Dhahir, K. Wheeler and H. He, *Chem. Commun.*, 2019, 4973–4976.
72 M. Gazvoda, M. Virant, B. Pinter and J. Košmrlj, *Nat. Commun.*, 2018, **9**, 4814.

73 R. Chinchilla and C. Nájera, *Chem. Soc. Rev.*, 2011, **40**, 5084–5121.

74 D.-L. Zhu, R. Xu, Q. Wu, H.-Y. Li, J.-P. Lang and H.-X. Li, *J. Org. Chem.*, 2020, **85**, 9201–9212.

75 M. Carril, A. Correa and C. Bolm, *Angew. Chem., Int. Ed.*, 2008, **47**, 4862–4865.

76 F. M. Moghaddam, G. Tavakoli and H. R. Rezvani, *Catal. Commun.*, 2015, **60**, 82–87.

77 Y. Liu, V. Blanchard, G. Danoun, Z. Zhang, A. Tlili, W. Zhang, F. Monnier, A. Van Der Lee, J. Mao and M. Taillefer, *ChemistrySelect*, 2017, **2**, 11599–11602.

78 F. Monnier, F. Turtaut, L. Duroure and M. Taillefer, *Org. Lett.*, 2008, **10**, 3203–3206.

79 A. Sagadevan and K. C. Hwang, *Adv. Synth. Catal.*, 2012, **354**, 3421–3427.

80 K. V. Arundhathi, P. Vaishnavi, T. Aneeja and G. Anilkumar, *RSC Adv.*, 2023, **13**, 4823–4834.

81 S. Diyarbakir, H. Can and Ö. Metin, *ACS Appl. Mater. Interfaces*, 2015, **7**, 3199–3206.

82 B. Wang, X. Guo, G. Jin and X. Guo, *Catal. Commun.*, 2017, **98**, 81–84.

83 A. Elhage, A. E. Lanterna and J. C. Scaiano, *ACS Sustainable Chem. Eng.*, 2018, **6**, 1717–1722.

84 G. S. More, A. K. Kar and R. Srivastava, *Inorg. Chem.*, 2022, **61**, 19010–19021.

85 P. Singh and A. C. Shaikh, *Chem. Commun.*, 2023, **59**, 11615–11630.

86 M. Shanmugam, A. Sagadevan, V. P. Charpe, V. K. K. Pampana and K. C. Hwang, *ChemSusChem*, 2020, **13**, 287–292.

87 S. Zhang and L. Zhao, *Nat. Commun.*, 2019, **10**, 4848.

88 A. Bakhoda, O. E. Okoromoba, C. Greene, M. R. Boroujeni, J. A. Bertke and T. H. Warren, *J. Am. Chem. Soc.*, 2020, **142**, 18483–18490.

89 S. Zhang and L. Zhao, *Nat. Commun.*, 2023, **14**, 6741.

90 S. Nematulloev, A. Sagadevan, B. Alamer, A. Shkurenko, R. Huang, J. Yin, C. Dong, P. Yuan, K. E. Yorov, A. A. Karluk, W. J. Mir, B. E. Hasanov, M. Nejib Hedhili, N. M. Halappa, M. Eddaoudi, O. F. Mohammed, M. Rueping and O. M. Bakr, *Angew. Chem., Int. Ed.*, 2023, **62**, e202303572.

91 R. J. Enemærke, T. B. Christensen, H. Jensen and K. Daasbjerg, *J. Chem. Soc., Perkin Trans. 2*, 2001, 1620–1630, DOI: **10.1039/B102835A**.

92 M. Mansour, R. Giacovazzi, A. Ouali, M. Taillefer and A. Jutand, *Chem. Commun.*, 2008, 6051–6053, DOI: **10.1039/B814364A**.

93 S. Biswas, A. Pal, M. K. Jena, S. Hossain, J. Sakai, S. Das, B. Sahoo, B. Pathak and Y. Negishi, *J. Am. Chem. Soc.*, 2024, **146**, 20937–20944.

94 M. Majek and A. Jacobi von Wangelin, *Angew. Chem., Int. Ed.*, 2013, **52**, 5919–5921.

95 V. W.-W. Yam, K. Kam-Wing Lo and K. Man-Chung Wong, *J. Organomet. Chem.*, 1999, **578**, 3–30.

96 A. Sagadevan, A. Ragupathi and K. C. Hwang, *Angew. Chem., Int. Ed.*, 2015, **54**, 13896–13901.

97 A. Sagadevan, V. P. Charpe, A. Ragupathi and K. C. Hwang, *J. Am. Chem. Soc.*, 2017, **139**, 2896–2899.

98 A. Sagadevan, A. Ragupathi, C.-C. Lin, J. R. Hwu and K. C. Hwang, *Green Chem.*, 2015, **17**, 1113–1119.

99 J. E. Hein and V. V. Fokin, *Chem. Soc. Rev.*, 2010, **39**, 1302–1315.

100 H. C. Kolb, M. G. Finn and K. B. Sharpless, *Angew. Chem., Int. Ed.*, 2001, **40**, 2004–2021.

101 M. Meldal and C. W. Tornøe, *Chem. Rev.*, 2008, **108**, 2952–3015.

102 R. Ramkumar and P. Anbarasan, *Cu-Catalyzed Click Reactions in Copper Catalysis in Organic Synthesis*, 2020, pp. 177–207, DOI: **10.1002/9783527826445.ch9**.

103 C. W. Tornøe, C. Christensen and M. Meldal, *J. Org. Chem.*, 2002, **67**, 3057–3064.

104 V. V. Rostovtsev, L. G. Green, V. V. Fokin and K. B. Sharpless, *Angew. Chem., Int. Ed.*, 2002, **41**, 2596–2599.

105 L. Liang and D. Astruc, *Coord. Chem. Rev.*, 2011, **255**, 2933–2945.

106 X. Wang, B. Huang, X. Liu and P. Zhan, *Drug Discovery Today*, 2016, **21**, 118–132.

107 J. D. Megiatto, Jr. and D. I. Schuster, *J. Am. Chem. Soc.*, 2008, **130**, 12872–12873.

108 J. W. Lee, J. H. Kim, B.-K. Kim, W. S. Shin and S.-H. Jin, *Tetrahedron*, 2006, **62**, 894–900.

109 D. Döhler, P. Michael and W. H. Binder, *Acc. Chem. Res.*, 2017, **50**, 2610–2620.

110 J. Chen, J. Wang, K. Li, Y. Wang, M. Gruebele, A. L. Ferguson and S. C. Zimmerman, *J. Am. Chem. Soc.*, 2019, **141**, 9693–9700.

111 C. Yang, J. P. Flynn and J. Niu, *Angew. Chem., Int. Ed.*, 2018, **57**, 16194–16199.

112 G. Oyman Eyrilmez, S. Doran, E. Murtezi, B. Demir, D. Odaci Demirkol, H. Coskunol, S. Timur and Y. Yagci, *Macromol. Biosci.*, 2015, **15**, 1233–1241.

113 The Nobel Prize in Chemistry, 2022, **https://www.nobelprize.org/prizes/chemistry/2022/popular-information/**.

114 K. Matyjaszewski, W. Jakubowski, K. Min, W. Tang, J. Huang, W. A. Braunecker and N. V. Tsarevsky, *Proc. Natl. Acad. Sci. U. S. A.*, 2006, **103**, 15309–15314.

115 K. Min, H. Gao and K. Matyjaszewski, *Macromolecules*, 2007, **40**, 1789–1791.

116 G. S. Kumar and Q. Lin, *Chem. Rev.*, 2021, **121**, 6991–7031.

117 M. A. Tasdelen and Y. Yagci, *Angew. Chem., Int. Ed.*, 2013, **52**, 5930–5938.

118 M. A. Tasdelen and Y. Yagci, *Tetrahedron Lett.*, 2010, **51**, 6945–6947.

119 B. J. Adzima, Y. Tao, C. J. Kloxin, C. A. DeForest, K. S. Anseth and C. N. Bowman, *Nat. Chem.*, 2011, **3**, 256–259.

120 Y.-Q. Xiao, P. Shang, X.-Y. Chen, X.-Q. Pu, K.-W. Jiang and X.-F. Jiang, *Chem. Mater.*, 2024, **36**, 2027–2038.

121 T. Yang, J. Jia, L. Xiong, S. Jin and M. Zhu, *Chem. Commun.*, 2024, **60**, 9614–9617, DOI: **10.1039/D4CC03288H**.

122 C. Dong, R.-W. Huang, A. Sagadevan, P. Yuan, L. Gutiérrez-Arzaluz, A. Ghosh, S. Nematulloev, B. Alamer, O. F. Mohammed, I. Hussain, M. Rueping and O. M. Bakr, *Angew. Chem., Int. Ed.*, 2023, **62**, e202307140.

123 L.-J. Liu, M.-M. Zhang, Z. Deng, L.-L. Yan, Y. Lin, D. L. Phillips, V. W.-W. Yam and J. He, *Nat. Commun.*, 2024, **15**, 4688.

124 N. Hoffmann, *Chem. Rev.*, 2008, **108**, 1052–1103.

125 A. W. Girotti, *J. Lipid Res.*, 1998, **39**, 1529–1542.

126 M. Cao, R. Pang, Q.-Y. Wang, Z. Han, Z.-Y. Wang, X.-Y. Dong, S.-F. Li, S.-Q. Zang and T. C. W. Mak, *J. Am. Chem. Soc.*, 2019, **141**, 14505–14509.

127 C. Zhang, Z. Wang, W.-D. Si, L. Wang, J.-M. Dou, Z.-Y. Gao, C.-H. Tung and D. Sun, *ACS Nano*, 2022, **16**, 9598–9607.

128 C. Zhu, Z.-L. Chen, H. Li, L. Lu, X. Kang, J. Xuan and M. Zhu, *J. Am. Chem. Soc.*, 2024, **146**, 23212–23220.

129 M. Bodiuzzaman, K. Murugesan, P. Yuan, B. Maity, A. Sagadevan, N. Malenahalli, H. S. Wang, P. Maity, M. F. Alotaibi, D.-E. Jiang, M. Abulikemu, O. F. Mohammed, L. Cavallo, M. Rueping and O. M. Bakr, *J. Am. Chem. Soc.*, 2024, **146**, 26994–27005.